Flying Capacitor Multicell Converter Based DVR with Energy Minimized Compensation Strategy

Seyed Hossein Hosseini[1], Arash Khoshkbar Sadigh[1], Ali Farshchi Tabrizi[1] and Gevorg Gharehpetian[2]

[1] Faculty of Electrical and Computer Engineering, University of Tabriz, Tabriz, Iran
hosseini@tabrizu.ac.ir , a.khoshkbar.sadigh@gmail.com , ali_farshchi@yahoo.com
[2] Electrical Engineering Department, Amirkabir University of Technology, Tehran, Iran
grptian@cic.aut.ac.ir

Abstract

One of the major power quality problems in distribution systems are voltage sags. This paper deals with a dynamic voltage restorer (DVR) as one of the different solutions to compensate these sags and protect sensitive loads. However, the quality of DVR output voltage, such as THD, is important. This paper present a new configuration of DVR based on flying capacitor multicell (FCM) converter. The main properties of FCM converter, which causes increase in the number of output voltage levels, are transformer-less operation and natural self-balancing of flying capacitors voltages. To avoid any exchange of active power in compensation process, the proposed DVR is controlled by energy minimized compensation strategy which is explained in details for general unbalanced voltage sags. Also, the proposed voltage sag detection method as well as proposed DVR reference voltage determination method based on synchronous reference frame (SRF) is adopted as the control system. The proposed DVR is simulated using PSCAD/EMTDC software and simulation results are presented to validate its effectiveness.

1. Introduction

Recently, an increased number of sensitive loads have been integrated into the electrical power systems. Consequently, the demand for high power quality and voltage stability has increased significantly. One serious threat for sensitive equipments in present grids is voltage sags [1]-[7]. These sags occur due to, *e.g.,* short circuits in the grid, inrush currents involved with the starting of large machines, or switching operations in the grid [5], [6].

The use of a DVR is one of the most effective solutions for "restoring" the quality of voltage at its load-side terminals when the quality of voltage at its source-side terminals is disturbed [1]-[8]. A traditional DVR mainly consists of series and shunt converters connected back-to-back and a common dc capacitor used as an energy-storage element [6], [8], [9]. The DVR injects three-phase compensating voltages in series to the power line. The energy required for the compensation of voltage sags is taken from the dc capacitor [7], [10], or another energy-storage element such as a double-layer capacitor, a superconducting magnet [11], or a lead-acid battery [12].

To avoid any exchange of active power between the DVR and power system in compensation process, energy minimized compensation (EMC) strategy concept has been proposed [4], [7], [10]. The EMC strategy is based on maximizing the active power delivered by the supply mains and the reactive power handled by the DVR during voltage sag. This can greatly reduce the required capacity of the energy storage device and thus, enhances the ride-through capability.

Numerous circuit topologies are available for the DVR [10]. The most common are the two- or three-level three-phase converter where the dc-side capacitor(s) is connected alternately to all ac phases. The purpose of this capacitor is to mainly absorb harmonic ripple and, hence, it has a relatively small energy storage requirement.

The (FCM) converter [13], [14], has many attractive properties for medium voltage applications including, in particular, the advantage of transformer-less operation and the ability to naturally maintain the flying capacitors voltages at their target operating levels. This important property is called natural self-balancing and allows the construction of such converters with a large number of voltage levels [13], [14]. However, the FCM converter based DVR configuration has not been proposed yet. Because of mentioned properties, in this paper a novel configuration of DVR based on 7-level FCM converter is proposed. Also, the EMC strategy is applied to DVR to compensate the voltage sags and a new synchronous reference frame (SRF) based voltage sag detection method and DVR reference voltage determination strategy are proposed which results in a good dynamic response time of the DVR. Simulation results are presented to validate the effectiveness and advantages of the novel configuration of DVR and its proposed methods of voltage sag detection and DVR reference voltage determination.

2. Proposed FCM Converter Based DVR

A typical DVR for voltage sag compensation is shown in Fig. 1. When the supply-side voltage changes the DVR injects a series voltage to maintain the magnitude of the load voltage at its reference value. The DVR is essentially a voltage-source converter that produces an ac output voltage and injects it in series with the supply voltage.

Note that the voltage injection also results in the supply of real and reactive power. Reactive power can be supplied without taking energy from the dc-side capacitor; however, an active power supply must involve the transfer of stored energy. Because of that, minimizing injected active power is attractive.

The series converter consists of a three-phase voltage-source converter or three single-phase voltage-source converters. It starts to inject three single-phase compensating voltages in series into the power line as soon as voltage sag occurs.

In this paper, the configuration of DVR based on the FCM converter is proposed. A 7-level FCM converter is shown in Fig. 2. The attractive properties of FCM converter are transformer-less operation, the natural self-balancing ability and increasing (redundancy) the number of combinations required to obtain a

desired voltage level.

As shown in Fig. 2, there are two dc capacitors for dc link of each single phase FCM converter, therefore for three single-phase FCM converters, six dc capacitors are required. While, as shown in Fig. 3, in this configuration only one dc link is used for three single-phase FCM converters. As a result, the required dc capacitors for dc link are decreased from 6 to 2.

For producing 7-level output voltage with the cascade multicell (CM) converter and only one dc link capacitor, it is essential to use three CM converters for each phase. Also, because of existence of only one dc link capacitor, it is required to use three isolation transformers for each phase. While in the same conditions, using an FCM converter causes to reduce the number of isolation transformers for each phase from 3 to 1. As a result, the cost, size and power loss of the DVR is decreased.

3. Control Strategies

Flying Capacitor Multicell Converter Control Strategy

Self-balancing of the flying capacitors voltages occurs naturally without any feedback control. A necessary condition for self-balancing is that the average flying capacitors currents must be zero. As a result, each cell must be controlled with the same duty cycle and a regular Phase Shifted Pulse Width Modulation (PSPWM) in which the phase shift between the carriers of each cell is:

$$\phi = 2\pi / n \qquad (1)$$

where, n is the number of cells. The PSPWM for the 7-level FCM converter is shown in Fig. 4.

Generally, an output RLC filter (balance booster circuit) is needed to accelerate the self-balancing process. This filter, which consists of a resistance, inductance and a capacitance connected in series, accelerates the self balancing process and is connected in parallel with the load. The output RLC filter is tuned to the switching frequency as follows:

$$\sqrt{L \cdot C} = \frac{1}{2 \cdot \pi \cdot f_{SW}} \qquad (2)$$

where, f_{SW} is the switching frequency, L and C are inductance and capacitance of the output RLC filter, respectively.
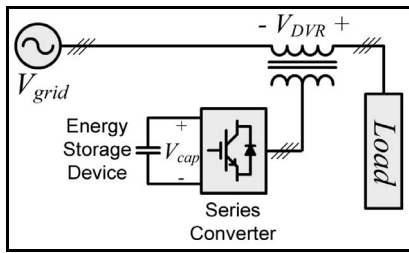
Fig. 1. Schematic diagram of DVR.
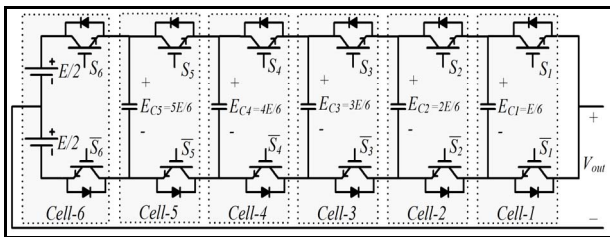
Fig. 2. Configuration of 7-level flying capacitor multicell converter.

Voltage Sags Compensation Strategy

To avoid tripping of the load, the amplitude of the load voltage has to be restored by the DVR. Different strategies can be used to achieve this goal. Three basic strategies are the pre-sag compensation [5], [15], in-phase compensation [4], [6] and the energy minimized compensation strategies [4], [7], [10]. In this paper, to avoid any exchange of active power in compensation process, the proposed DVR is controlled by EMC strategy which is described as following.

One of existing strategy to compensate the voltage sag is injecting as much reactive power as possible to compensate the sag. Therefore, the DVR voltage must be controlled in such a way that the DVR does not exchange the active power with power system. Compensating voltage sags with pure reactive power is possible as long as the voltage sag is quite shallow and therefore, the compensation time is not limited. The phasor diagram of the EMC strategy is shown in Fig. 5. In this figure, the dashed quantities (V'_{grid}, V'_{load}, V'_{dvr} and I'_{load}) indicate variables after the sag. The phasors prior to the sag are represented by V_{grid}, V_{load} and I_{load}. All of the load and grid voltage phasors are line-neutral voltages.

In this paper, the EMC strategy is explained in details for unbalanced voltage sags which can also be used for any kind of voltage sags. In the unbalanced voltage sags which are so practical, it is assumed that the variations of voltage phase angle and amplitude in each phase are different. In this condition, the angle of α (as shown in Fig. 5) is calculated by making the required active power of DVR equal to zero as follows:

$$P_{DVR} = P_{load} - P_{grid} = 0 \qquad (3)$$

$$P_{load} = 3 \cdot V_{load} \cdot I_{load} \cdot \cos(\phi) \qquad (4)$$

$$P_{grid} = \sum_{k=a,b,c} \left[V'_{grid,k} \cdot I_{load} \cdot \cos\left(\phi - \alpha - \delta_k\right) \right] \qquad (5)$$

By substituting (4) and (5) into (3), it can be written as follows:

$$\alpha = \varphi - \lambda - \cos^{-1}\left(\frac{3 \cdot V_{load} \cdot \cos(\varphi)}{\sqrt{X^2 + Y^2}} \right) \qquad (6)$$

where,

$$X = \sum_{k=a,b,c} \left[V'_{grid,k} \cdot \cos(\delta_k) \right] \qquad (7)$$

$$Y = \sum_{k=a,b,c} \left[V'_{grid,k} \cdot \sin(\delta_k) \right] \qquad (8)$$

$$\lambda = \tan^{-1}\left(\frac{Y}{X} \right) \qquad (9)$$

According to (6), following condition:

$$3 \cdot V_{load} \cdot \cos(\varphi) \leq \sqrt{X^2 + Y^2} \qquad (10)$$

must be satisfied. Otherwise, the angle of α obtained from (11). In this condition, the required active power of DVR can not be zero.

$$\frac{d}{d\alpha}(P_{DVR}) = 0 \qquad (11)$$

According to (7) and (8), the rms and phase angle variation of each line-neutral grid voltage must be obtained from measured voltages during voltage sag occurrence in which each measured line-neutral grid voltage can be written as follows:

$$V'_{grid,k}(t) = \sqrt{2} \cdot \left| V'_{grid,k} \right| \cdot \sin\left(\omega t + \varphi - \delta_k\right) \qquad (12)$$
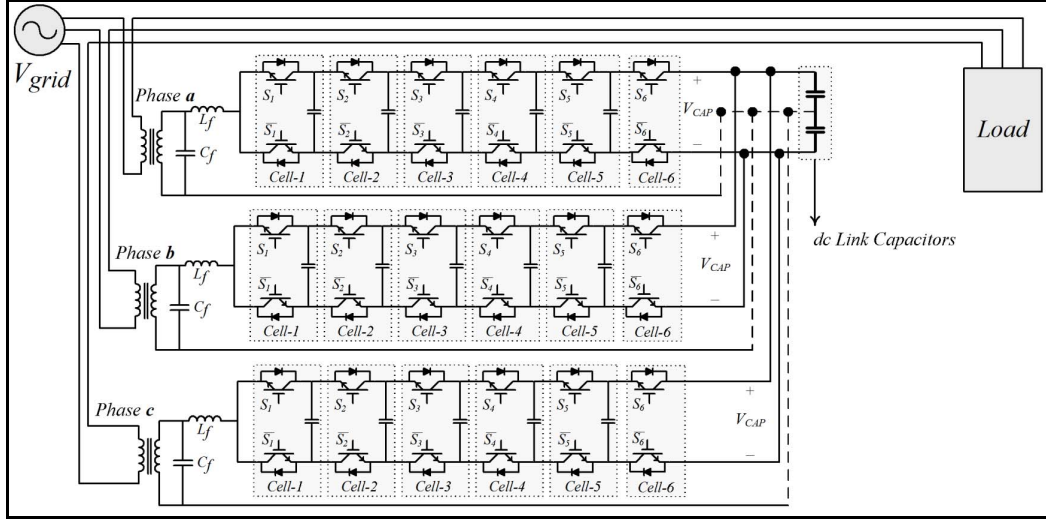
Fig. 3. Power circuit of the proposed DVR based on 7-level flying capacitor multicell converter.
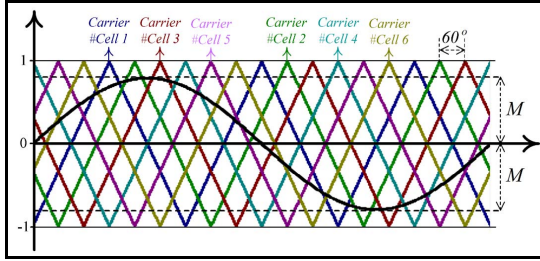
Fig. 4. Phase shifted pulse width modulation for 7-level flying capacitor multicell converter.

where, k represent each phase. In order to calculate the rms and phase angle variation of each line-neutral grid voltage, they can be transferred to SRF as follows:

$$\begin{bmatrix} f_\alpha(t) \\ f_\beta(t) \end{bmatrix} = \begin{bmatrix} 2\sin(\omega t) \\ 2\cos(\omega t) \end{bmatrix} \times f(t) \quad (13)$$

where, $f_\alpha(t)$ and $f_\beta(t)$ are the α and β components of signal $f(t)$. By substituting (12) in (13), the α and β components of each line-neutral grid voltage can be written as:

$$\left(V'_{grid,k} \right)_\alpha (t) = \sqrt{2} \cdot \left| V'_{grid,k} \right| \cdot \cos\left(\phi - \delta_k \right)$$
$$- \sqrt{2} \cdot \left| V'_{grid,k} \right| \cdot \cos\left(2\omega t + \phi - \delta_k \right) \quad (14)$$

$$\left(V'_{grid,k} \right)_\beta (t) = \sqrt{2} \cdot \left| V'_{grid,k} \right| \cdot \sin\left(\phi - \delta_k \right)$$
$$+ \sqrt{2} \cdot \left| V'_{grid,k} \right| \cdot \sin\left(2\omega t + \phi - \delta_k \right) \quad (15)$$

Now it is possible to extract the dc components from SRF isolator as:

$$v_{\alpha,k}(t)\big|_{dc} \equiv V_{\alpha,k} = \sqrt{2} \cdot \left| V'_{grid,k} \right| \cdot \cos\left(\phi - \delta_k \right) \quad (16)$$

$$v_{\beta,k}(t)\big|_{dc} \equiv V_{\beta,k} = \sqrt{2} \cdot \left| V'_{grid,k} \right| \cdot \sin\left(\phi - \delta_k \right) \quad (17)$$

therefore, the rms and phase angle variation of each line-neutral grid voltage which are calculated using (16) and (17) can be written as follows:

$$\left| V'_{grid,k} \right| = \sqrt{\left(V_{\alpha,k}{}^2 + V_{\beta,k}{}^2 \right)/2} \quad (18)$$

$$\delta_k = \phi - \arctan\left(\frac{V_{\beta,k}}{V_{\alpha,k}} \right) \quad (19)$$
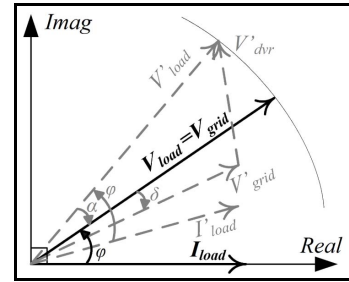
Fig. 5. Phasor diagram of the energy minimized compensation strategy.

4. Proposed Detection and Determination Strategies

In this paper, the SRF is proposed to detect the voltage sags and determine the DVR reference injected voltage. At the beginning, the voltage sag must be detected and then, the DVR reference injected voltage must be determined.

As the first step of voltage sag detection, the line-neutral grid voltages are measured and transferred from *abc* coordinate system to SRF as follows:

$$\begin{bmatrix} V_{grid,d} \\ V_{grid,q} \\ V_{grid,0} \end{bmatrix} =$$
$$\frac{2}{3} \begin{bmatrix} \cos(\omega t) & \cos(\omega t - 120) & \cos(\omega t + 120) \\ \sin(\omega t) & \sin(\omega t - 120) & \sin(\omega t + 120) \\ \frac{1}{2} & \frac{1}{2} & \frac{1}{2} \end{bmatrix} \cdot \begin{bmatrix} V_{grid,a} \\ V_{grid,b} \\ V_{grid,c} \end{bmatrix} \quad (20)$$

where, $V_{grid,a}$, $V_{grid,b}$, $V_{grid,c}$ are the measured line-neutral grid voltages of phases *a*, *b* and *c*, respectively and $V_{grid,d}$, $V_{grid,q}$, $V_{grid,0}$ are the *d*-component, *q*-component and *zero*-component of grid voltages in the SRF, respectively. Also, the rms value (line-neutral) of balanced grid voltage

$\left(\left|V_{grid}\right|\right)$ can be calculated using the d-component and q-component of grid voltages as follows:

$$\left|V_{grid}\right| = \frac{1}{\sqrt{2}}\sqrt{\left(V_{grid,d}\right)^2 + \left(V_{grid,q}\right)^2} \qquad (21)$$

Then, the phase angle of phase a voltage in the pre-sag state (healthy state) is stored as the reference angle as follows:

$$\theta^{ref} = \arctan\left(\frac{\left.V_{grid,d}\right|_{dc}}{\left.V_{grid,q}\right|_{dc}}\right) \qquad (22)$$

where, $\left.V_{grid,d}\right|_{dc}$ and $\left.V_{grid,q}\right|_{dc}$ are dc values of d and q-components of grid voltages in the SRF, respectively.

In the case of single phase voltage sag or unbalanced three phase voltage sag, the *zero*-component of grid voltages in the SRF is not nil. Therefore, it can be used as a parameter to detect the voltage sag. However, in the case of balanced three phase voltage sag, the *zero*-component of grid voltages in the SRF is nil and only the rms value of balanced grid voltage in the sag state changes. Because of that, it is necessary to use the obtained rms value of line-neutral grid voltages ($\left|V_{grid}\right|$) from (21) as another parameter to detect the voltage sag. Finally, the following proposed algorithm based on two steps is performed iteratively to detect the voltage sags:

Step-1: The zero-component of grid voltages in the SRF which is obtained from (20) is analyzed. If it is not equal zero, it means that the unbalanced voltage sag is occurred. So, the voltage sag is detected and then, quit the algorithm. If the *zero*-component is equal to zero, go to step-2. The nil *zero*-component means that the grid voltages are balanced. So, the rms value of grid voltages must be analyzed as step-2.

Step-2: The obtained rms value of line-neutral grid voltages ($\left|V_{grid}\right|$) from (21) is compared with the reference rms value of line-neutral grid voltages (V_{rms}^{ref}). If they are not equal to each other, it means that the voltage sag is occurred. So, the voltage sag is detected and then, quit the algorithm. If there is no difference between them, go to step-1.

Using the explained algorithm makes it possible to detect any balanced or unbalanced voltage sags. After the detection of voltage sags, the reference rms value of line-neutral grid voltages (V_{rms}^{ref}), the obtained reference angle (θ^{ref}) and the angle of α, obtained from (6), are used to determine the values of reference grid voltages in the SRF as follows:

$$V_{grid,d}^{ref} = \sqrt{2} \cdot V_{rms}^{ref} \cdot \sin\left(\theta^{ref} + \alpha\right) \qquad (23)$$

$$V_{grid,q}^{ref} = \sqrt{2} \cdot V_{rms}^{ref} \cdot \cos\left(\theta^{ref} + \alpha\right) \qquad (24)$$

where, $V_{grid,d}^{ref}$ and $V_{grid,q}^{ref}$ are the reference d and q-components of grid voltages in the SRF, respectively.

Next, the differences between the *dq0* values of line-neutral grid voltages and the *dq0* values of reference line-neutral grid voltages are taken into account as *dq0* values of DVR reference injected voltages as follows:

$$V_{dvr,d}^{ref} = V_{grid,d}^{ref} - V_{grid,d} \qquad (25)$$

$$V_{dvr,q}^{ref} = V_{grid,q}^{ref} - V_{grid,q} \qquad (26)$$

$$V_{dvr,0}^{ref} = -V_{grid,0} \qquad (27)$$

where, $V_{dvr,d}^{ref}$, $V_{dvr,q}^{ref}$ and $V_{dvr,0}^{ref}$ are the reference d-component, q-component and *zero*-component of DVR series injected voltages in the SRF, respectively. These values are transferred to *abc* coordinate system and then, three single-phase reference voltages of DVR are obtained as follows:

$$\begin{bmatrix} V_{dvr,a}^{ref} \\ V_{dvr,b}^{ref} \\ V_{dvr,c}^{ref} \end{bmatrix} = \begin{bmatrix} \cos(\omega t) & \sin(\omega t) & 1 \\ \cos(\omega t - 120) & \sin(\omega t - 120) & 1 \\ \cos(\omega t + 120) & \sin(\omega t + 120) & 1 \end{bmatrix} \cdot \begin{bmatrix} V_{dvr,d}^{ref} \\ V_{dvr,q}^{ref} \\ V_{dvr,0}^{ref} \end{bmatrix} \quad (28)$$

where, $V_{dvr,a}^{ref}$, $V_{dvr,b}^{ref}$ and $V_{dvr,c}^{ref}$ are the DVR reference injected voltages of phase a, b and phase c, respectively.

5. Simulation Results

Computer simulation is provided to verify the well-performance of the proposed DVR configuration as well as proposed voltage sag detection method and DVR reference voltage determination strategy. The parameters used in the simulation are given in TABLE I. The system is simulated using PSCAD/EMTDC software.

In Fig. 6, the simulation results are depicted in two periods. In first one the unbalanced voltage sag is occurred at the grid at $t = 0.12\ s$ while the grid voltages of phases a and b drop to 60% of their nominal values. In second period, the unbalanced voltage sag is occurred at $t = 0.2\ s$ while the grid voltage of phase a drops to 70% and the grid voltages of phases b and c drop to 80% of their nominal values. Additionally, a phase jump of -15 degrees is applied to the grid voltage of phase a.

As shown in Fig. 6, the proposed strategies are able to detect voltage sags as well as determine the three single-phase reference voltages of DVR and compensate long-duration unbalanced sags without delaying the suitable operation of proposed DVR. Considering the load voltage obtained from simulation results, it can be deduced that the compensation starts immediately when grid voltage sag is detected; also, the DVR shows a good response time for detection of voltage sag and compensating operation. As shown in Fig. 6(e), DVR absorbs small active power (considering $P_{load} = 2.3\ MW$) because of transformer and switching power losses; while, if DVR doesn't absorb this active power, the dc link capacitors must support power losses which cause to decrease voltage of dc link capacitors.

6. Conclusion

Voltage sags are major problems in power systems due to the increased integration of sensitive loads into them. DVR systems are able to compensate these voltage sags. Because the multicell converters are very interesting for high-power/medium-voltage applications, and also considerably improve the output voltage frequency spectrum, in this paper an FCM converter based DVR has been proposed to improve the quality of DVR output voltage. In the proposed configuration, only one dc link is used for three single-phase FCM converters. So, the required dc capacitors for dc link are decreased from 6 to 2.

Also, the detection and determination methods based on the SRF have been proposed to detect the voltage sag and determine the DVR reference series injected voltage. As depicted in simulation results, the energy minimized compensation strategy and the proposed SRF based detection and determination methods show excellent performance and good dynamic response time.
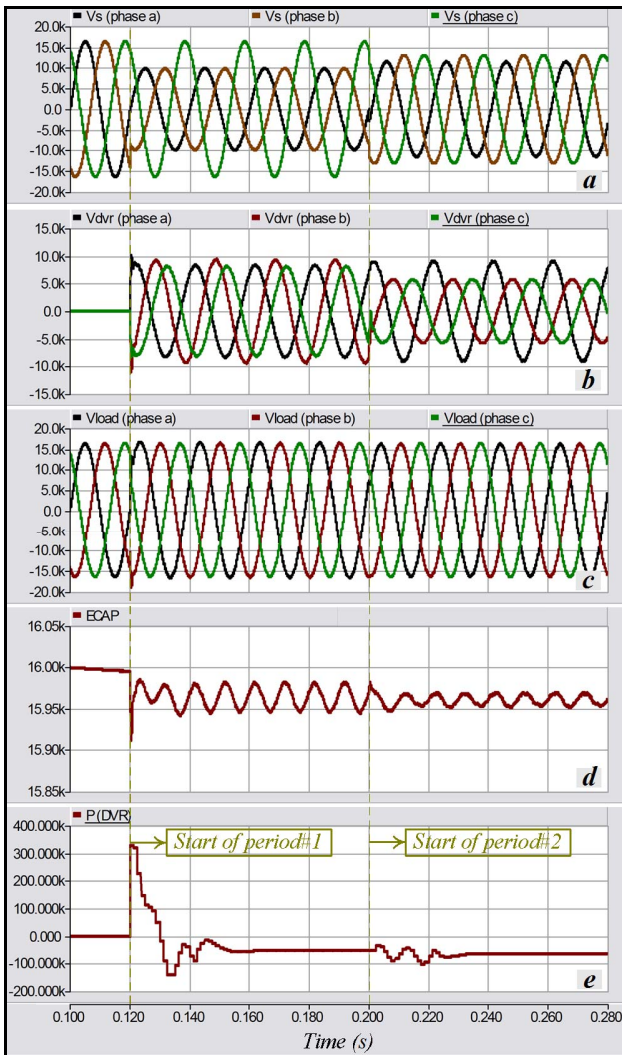
Fig. 6. Simulation results: a) grid voltage (Volt); b) DVR injected voltage (Volt); c) load voltage (Volt); d) dc link voltage (Volt); e) DVR active power (Wat).

Table 1. Parameters of simulated system

System Parameters	Values
Capacitor used in DC link (mF)	4
Flying capacitors used in flying capacitor multicell converter (μF)	200
Output RLC filter tuned to f_{SW} R (Ω), L (mH), C (μF)	50;0.1;2.
Output RLC filter tuned to $2f_{SW}$ R (Ω), L (mH), C (μF)	50;0.025; 2.5
Inductance and capacitance of output series filter	1;30
Turn ratio of isolation series transformers	0.7
Resistance & inductance of load R (Ω), L (H)	50 ; 0.25

7. References

[1] M.R. Banaei, S.H. Hosseini and G.B. Gharehpetian, "Inter-line dynamic voltage restorer control using a novel optimum energy consumption strategy", *Elsevier Journal of Simulation Modeling Practice and Theory*, vol. 14, no. 7, pp. 989–999, Oct. 2006.

[2] M.R. Banaei, S.H. Hosseini, S. Khanmohamadia and G.B. Gharehpetian, "Verification of a new energy control strategy for dynamic voltage restorer by simulation", *Elsevier Journal of Simulation Modeling Practice and Theory*, vol. 14, no. 2, pp. 112–125, Feb. 2006.

[3] E. Babaei, S.H. Hosseini, G.B. Gharehpetian, M. Tarafdar Haquea and M. Sabahi, "Reduction of dc voltage sources and switches in asymmetrical multilevel converters using a novel topology", *Elsevier Journal of Electric Power Systems Research*, vol. 77, no. 8, pp. 1073–1085, Jun. 2007.

[4] C. Ngai-man Ho, H. S. H. Chung and K. T. K. Au, "Design and implementation of a fast dynamic control scheme for capacitor-supported dynamic voltage restorers", *IEEE Trans. Power Electronics*, vol. 23, no. 1, pp. 237–251, Jan. 2008.

[5] P. R. Sánchez, E. Acha, J. E. O. Calderon, V. Feliu and A. G. Cerrada, "A Versatile control scheme for a dynamic voltage restorer for power-quality improvement", *IEEE Trans. Power Delivery*, vol. 24, no. 1, pp. 277–284, Jan. 2009.

[6] B. Wang and G. Venkataramanan, "Dynamic voltage restorer utilizing a matrix converter and flywheel energy storage", *IEEE Trans. Industry Applications*, vol. 45, no. 1, pp. 222–231, Jan./Feb. 2009.

[7] H. K. Al-Hadidi, A. M. Gole and D. A. Jacobson, "A Novel configuration for a cascade inverter based dynamic voltage restorer with reduced energy storage requirements", *IEEE Trans. Power Delivery*, vol. 23, no. 2, pp. 881–888, Apr. 2008.

[8] S. A. Saleh, C. R. Moloney and M. A. Rahman, "Implementation of a dynamic voltage restorer system based on discrete wavelet transforms", *IEEE Trans. Power Delivery*, vol. 23, no. 4, pp. 2366–2375, Oct. 2008.

[9] C. S. Lam, M. C. Wong, and Y. D. Han, "Voltage swell and over-voltage compensation with unidirectional power flow controlled dynamic voltage restorer", *IEEE Trans. Power Delivery*, pp. 1–9, in press.

[10] H. K. Al-Hadidi, A. M. Gole and D. A. Jacobson, "Minimum power operation of cascade inverter based dynamic voltage restorer", *IEEE Trans. Power Delivery*, vol. 23, no. 2, pp. 889–898, Apr. 2008.

[11] J. Lamoree, L. Tang, C. DeWinkel, and P. Vinett, "Description of a micro-SMES system for protection of critical customer facilities", *IEEE Trans. Power Delivery*, vol. 9, no. 2, pp. 984–991, Apr. 1994.

[12] V. K. Ramachandaramurthy, C. Fitzer, A. Arulampalam, C. Zhan, M. Barnes and N. Jenkins, "Control of a battery supported dynamic voltage restorer", *Proc. Inst. Electr. Eng.—Generation, Transmission Distrib.*, Sep. 2002, vol. 149, no. 5, pp. 533–542.

[13] S. H. Hosseini, A. Khoshkbar Sadigh and A. Sharifi, "Estimation of flying capacitors voltages in multicell converters", in *Proc. 6th international conference Electrical Engineering/Electronics, Computer, Telecommunications and Information Technology (ECTI)*, Pattaya, Thailand, May 2009, pp. 110–113.

[14] B. P. McGrath, T. Meynard, G. Gateau and D. G. Holmes, "Optimal modulation of flying capacitor and stacked multicell converters using a state machine decoder", *IEEE Trans. Power Electronics*, vol. 22, no. 2, pp. 508-516, Mar. 2007.

[15] J. G. Nielsen and F. Blaabjerg, "Control strategies for dynamic voltage restorer compensating voltage sags with phase jump," in *Proc. Annu. Appl. Power Electronics Conf. Exposition*, 2001, no. 2, pp. 1267–1273.